Agronomy Research **19**(S1), 749–766, 2021
https://doi.org/10.15159/AR.21.057

Waste fish oil as an alternative renewable fuel for IC engines

M. Hissa*, S. Niemi, T. Ovaska and A. Niemi

University of Vaasa, School of Technology and Innovations, P.O. Box 700, FI-65101 Vaasa, Finland
*Correspondence: Michaela.Hissa@univaasa.fi

Received: January 31st, 2021; Accepted: April 10th, 2021; Published: April 30th, 2021

Abstract. Bio-oils are potential fuels for internal combustion engines because of they have advantageous properties such as biodegradability, renewability, high oxygen content and low sulphur. However, the high viscosity, surface tension, and density of crude bio-oils pose challenges for engine use. Those properties affect fuel spray characteristics, mixture formation and combustion. In turn, these impact engine, efficiency, power and emissions. This study investigated the use of crude fish oil (FO) at medium and low engine-loads at two engine speeds in an off-road engine. The injectors had 6-hole high flow rate tips. The results were compared with those of fossil diesel fuel oil (DFO). Fish oil increased hydrocarbon (HC), carbon monoxide (CO) and partly oxides of nitrogen (NOx) emissions. Smoke number, however, decreased. Crude fish oil also showed lowered total particle number (TPN) at low load at low engine-speed compared with DFO.

Key words: diesel engine, bio-oil, combustion, gaseous emissions, particle number.

INTRODUCTION

Bio-based fuels can provoke economic, social, and environmental issues, especially if the raw material used in their production is edible. Consequently, the focus for biofuel production is switching to alternative raw materials such as non-edible vegetable oils, used cooking oils, fatty acids from algae, and animal fats (Sirviö, 2018; Ching-Velasquez et al., 2020).

According to its 2019 Government Programme, Finland will be carbon-neutral by 2035 (Ministry of the Environment, 2019). The already standardised blends of biodiesel and fatty acid methyl ester (FAME) fuels are one realistic way to increase the share of renewables to fulfil Finnish government and European Union targets (Sirviö, 2018). Many Finnish farms and factories are willing to increase the self-sufficiency of their energy production by utilising waste materials like crude fish oil as a fuel feedstock (Niemi et al., 2009; Niemi et al., 2011).

The crude oil extracted from discarded parts of marine fish may provide an abundant, cheap and stable source of raw oil to allow maritime countries to produce biodiesel and help to reduce pollutant emissions (Lin & Li, 2009; de Almeida et al., 2015). However, diesel engines can burn even unrefined bio-oils, such as animal fats, vegetable oils, and waste oils. This increases the interest in crude bio-oils (Niemi et al.,

2009; Niemi et al., 2011; Hoang, 2019). The use of straight bio-oils with minimal refining should even be preferable since refining always consumes energy and adds carbon dioxide (CO_2) emissions (Niemi et al., 2009; Esteban et al., 2012). Power plants with medium-speed engines fuelled by neat bio-oil are already in operation around the world (Ollus & Juoperi, 2007; Niemi et al., 2011).

World fish production in 2018 was around 179 million tonnes, of which 12% was used for non-food purposes (Food and Agriculture Organization of the United Nations, FAO, 2020). More efficient and sustainable use of fisheries and aquaculture production must be implemented since a large proportion - as much as 35% - of production is either lost or wasted. Improvements can be achieved through appropriate policies, regulatory frameworks, capacity building, services and infrastructure, as well as physical access to markets. (FAO, 2020).

Most of the fish oil is used in the cosmetic, pharmaceutical, and human dietary complement industries (Bruun, 2019). If the fish oil degrades during storage or handling it can be used in marine or stationary diesel engines (Bruun, 2019). The oil can be also processed further to produce biodiesel. Thus, there is already large potential to also use fish wastes for fuel production.

Crude bio-oils have shown several advantages as fuels in IC engines. Compared with DFO, many studies report a significant reduction of toxic emissions and noise; small or insignificant generation of greenhouse gas (GHG) emissions; and lower emissions of NOx, polycyclic aromatic hydrocarbons (PAHs), particulate matter (PM) and smoke (How et al., 2012; Satyanarayana & Muraleedharan, 2012; Hoang, 2019).

Although liquid biofuels are a good alternative to fossil fuel oil, there are challenges associated with their use. For example, studies by, Niemi et al. (2011), Deshmukh et al. (2012), Fan et al. (2014), and Sirviö (2018) conclude that the high viscosity of neat bio-oils affects fuel atomisation and efficient combustion. They point to specific issues of large droplet size, long spray penetration, formation of deposits, injector coking, ring sticking, piston seize-up, lube oil dilution, filter choking etc. Other limiting factors for the use of pure bio-oils are their lower heating value and cetane number, higher density and surface tension when compared to DFO, as well as their acidic and corrosive properties, plus their water and oxygen (How et al., 2012; Bruun, 2019; Hoang, 2019). Studies by Hoang, (2019), Rakopoulos et al. (2014) and Chauhan et al. (2010) report that crude bio-oils give reduced power output but more deposit formation in the combustion chamber and injector holes, resulting in increased carbon monoxide (CO) and unburnt hydrocarbon (HC) emissions.

Unlike FAME biodiesels, crude bio-oils do not have common quality specifications. Some producers have their own specifications that set limits for viscosity, density, water content, acid number, sulphur content etc. These limits are based on the experiences of using bio-oils in diesel engines (Bruun, 2019). For example, according to Ollus & Juoperi (2007), the acid number of crude bio-oils should be below 5.0 mg KOH g^{-1}; the water content less than 0.20% (V V^{-1}); the sulphur content less than 500 ppm; and phosphorus content below 100 ppm.

The main research question of the current study was whether fish oil from left-over fish trimmings could be used as an alternative fuel in the local fishermen's vessels. The study was part of a project that investigated the potential to make more efficient use of fish trimmings and by-catches in Ostrobothnia, Finland (Skog et al., 2013). The present study investigated the use of crude fish oil in a high-speed, common-rail diesel engine

equipped with 6-hole injector nozzles with high flow rates. The engine was driven at three loads and at two speeds. The results were compared to those when fuelling with DFO. All the engine parameters were unchanged. The measurements provide new information on the suitability of crude fish oil for a high-speed, off-road engine, particularly with regard to total exhaust particle numbers (TPN). The results support and promote the more efficient use of renewable fuels in an ICE.

MATERIALS AND METHODS

Experimental setup

The University of Vaasa (UV) conducted the experiments at the Internal Combustion Engine (ICE) laboratory of the Technobothnia laboratory unit in Vaasa, Finland.

Engine setup

The experimental engine, an AGCO Power 44 CWA, was a turbocharged and intercooled, high-speed, four-cylinder diesel engine for non-road applications. It had a Bosch common-rail fuel injection system but no exhaust gas after-treatment. The engine was loaded by means of a Horiba WT300 eddy-current dynamometer. The main specification of the engine is given in Table 1.

Table 1. Main engine specification

Engine	AGCO POWER 44 CWA
Cylinder number	4
Bore (mm)	108
Stroke (mm)	120
Swept volume (dm^{-3})	4.4
Rated speed (min^{-1})	2,200
Rated power (kW)	96
Intermediate speed (min^{-1})	1,500

The current study was an extension to the research of how selected fuel injection nozzles affect the injection, combustion, and emission characteristics of a modern high-speed common-rail diesel engine (Hissa et al., 2020). That study compared solenoid-driven injectors with 6-, 8- or 10-hole nozzles. The 6-hole injector nozzles were selected for use with the crude fish oil because the larger orifices of the 6-hole nozzles were more suited to the high-viscosity FO. Three different engine loads were used. Loads of 50% and 25% were applied at engine speed of 1,500 min^{-1} (intermediate speed): a 10% load was applied at the engine's rated speed of 2,200 min^{-1}. The nozzles had a high mass flow rate (1.2 L min^{-1} at 100 bar) and the spray angle was 149°. Most diesel combustion systems use spray angles in the range of 145°–158°. The engine manufacturer optimised the injection map for the 8-hole nozzles, but the same map was used with these alternative 6-hole nozzles. Table 2 gives the specifications of the 6- and 8-hole nozzles.

Table 2. Specifications of the 6- and 8-hole injector nozzles

Number of nozzle holes	6	8
Orifice diameter (mm)	0.2	0.162
Total orifice areas (mm^2)	0.188	0.165
Included spray angle	149°	149°
Nozzle flow rate (L min^{-1}) at 100 bar	1.2	1.2

Physical properties of test liquids

The baseline fuel was a commercial low-sulphur diesel fuel oil (DFO). The unprocessed crude fish oil (FO) was purchased from Storfjärdens Fisk Ab, Åland (Aland Islands), Finland. Table 3 lists the key properties of the studied fuels.

FO contained saturated fatty acids (SAF) 18.0%; monounsaturated fatty acids (MUF) 43.9%; and polyunsaturated fatty acids (PUF) 37.4%. The extended measurement uncertainty for fatty acids was ± 16%. The fatty acid composition is related to the viscosity of a fuel. Fuel viscosity value decreases with the increase in the amount of unsaturated fatty acids (Ching-Velasquez et al., 2020; Deshmukh et al., 2012, Esteban et al., 2012).

The concentration of double carbon bonds (MUF or PUF) has also been found to affect carbon deposit formation in engines (Bruun et al., 2019). Jayasinghe et al. (2012) state that the key challenge for the feasibility of fish oil as a fuel is the recovery of the oil from the waste. A high PUF content decreases the thermal and oxidation stability of the fish waste. This needs to be taken into consideration when managing the storage and transport of fish waste.

Table 3. Fuel properties

	Unit	DFO	Fish oil
Carbon content	wt-%	86.1	77.2
Hydrogen content	wt-%	13.7	11.5
Nitrogen content	wt-%	0.19	0.13
Sulphur content	mg kg^{-1}	3.3	2.1
Ash content (775 °C)	wt-%	< 0.001	< 0.001
Cetane number, IQT	-	54	*
LHV	MJ kg^{-1}	43	37
Density at 15 °C	kg m^{-3}	835	920
Acid number	mg KOH g^{-1}	-	2.09
Kin. viscosity at 40 °C	mm^2 s^{-1}	3**	28**
Iodine value	g $100g^{-1}$	-	132
Water content	mg kg^{-1}	< 200**	909
Surface tension	mN m^{-1}	28.5	33.6
Oxidation stability	h	-	0.68

*Fish oil was too viscous for measuring cetane number; ** Literature value (Niemi et al., 2009).

The acid number (AN) for FO was 2.09 mg KOH g^{-1}. This is substantially lower than literature values: for example, Bruun et al. (2019) reported AN values of 17–25 mg KOH g^{-1} for fish oils. The acids in bio-oils increase the corrosion risk and in the long term shorten the expected lifetime of certain engine components, notably the fuel injection system. AN above 100 mg KOH g^{-1} is considered definitely corrosive. AN below 5 mg KOH g^{-1} is defined as not to increase the corrosion risk (Ollus & Juoperi, 2007). Specifically, fish oils are reported to have high AN due to the presence of water and PUF that are more susceptible to oxidation and free fatty acid formation (Ching-Velasquez et al., 2020). With an AN value well below 5 mg KOH g^{-1}, the fish oil in this study does not pose a corrosion risk.

In literature, the kinematic viscosity value of crude fish oil has been measured at 28 mm^2 s^{-1} (Niemi et al., 2009), and that of DFO at 3 mm^2 s^{-1}. FO's high viscosity hinders the production of a fine fuel spray using a practical fuel nozzle. High viscosity modifies the droplet distribution due to the formation of larger droplets. Fuel viscosity increases sharply in cold conditions, which may cause restrictions in fuel delivery that result in the reduction of the volumetric flow (Bosch, 2018). Adjusting the fish oil temperature can compensate for its higher viscosity compared to traditional fuels (Bruun et al., 2019).

The density of FO in this study was 920 kg m^{-3}. Fuel density affects the dispersion of the fuel injected into the cylinder. Higher density increases compression ratio, the mass of fuel injected and fuel droplet diameter. These have a direct impact on injection timing and injection spray pattern. Increased density reduces fuel atomisation and

mixing with air: this reduction is associated with higher PM and NOx emissions. According to a manufacturer of marine diesel engines, the density of liquid biofuel should be lower than 991 kg m^{-3} for four-stroke engines (Juoperi & Ollus, 2008; Jayasinghe et al., 2012).

FO was too viscous to measure its cetane number (CN) by an ignition quality tester (IQT). In the study of Niemi et al. (2011) CN for crude fish oil was 49, i.e., not very low. In the current study, DFO had a CN of 54. CN has an impact on the ignition delay (ID). A low CN increases ID, resulting in poorer combustion and leading to noise and smoke emissions (Hissa et al., 2018).

The LHV (lower heating value) of FO (37 MJ kg^{-1}) is substantially less than that of the DFO (43 MJ kg^{-1}), thus increasing the required fuelling rate to achieve the same engine power output (Drenth et al., 2014). The presence of water in fish oil decreases its heating value. FO had high water content: over 900 mg kg^{-1}. In engine use, water in oil may cause corrosion of the equipment and containers (Adeoti & Hawboldt, 2015; Bruun et al., 2019).

If the same volume of two fuels, with different fuel densities, are injected to an engine, the fuel with higher density provides higher engine output. However, this occurs only if lower heating values (LHV) do not differ greatly. (Murtonen, 2004) Since in this study, the density of fish oil is significantly greater than that of diesel, the energy per injection is actually more similar than based on LHV alone.

The surface tension of FO was 18% higher than that of diesel. Surface tension has a direct impact on the size of fuel droplets, so FO's higher surface tension might also contribute to an increase in its droplet diameters (Heywood, 2018).

Analytical instruments

LabVIEW system-design software was used to collect the sensor data from the engine. The recorded variables were engine speed and torque, cylinder pressure and injection timing, duration, and quantity. A WinEEM3 program provided by the engine manufacturer, AGCO Power, controlled fuel injection according to load-speed requests. The basic settings of WinEEM3 were the same for all nozzles and fuels. Fig. 1 is a schematic of the test bench setup.

A piezoelectric Kistler 6125C pressure sensor measured the in-cylinder pressure. The sensor was mounted on the head of the fourth cylinder. A charge amplifier filtered and amplified the signal, which was then transmitted to a Kistler KIBOX combustion analyser. The crankshaft position was recorded by a crank-angle encoder (Kistler 2614B1), which can output a crank-angle signal with a resolution of 0.1 °CA by means of an optical sensor. The cylinder-pressure data was averaged over 100 consecutive cycles to smooth irregular combustion. The averaged data were used to calculate the heat release rate (HRR).

The HRR and mass fraction burned (MFB) were calculated via AVL Concerto's data-processing platform, using the Thermodynamics2 macro. The macro used a calculation resolution of 0.2 °CA. The start of the calculation was set at -30 °CA. The data were filtered with the DigitalFilter macro and a frequency of 2000 Hz. For the HRR results, the average values of in-cylinder pressure were calculated first. Thereafter, the macro was used to calculate HRR values. Finally, the HRR curve was filtered. In contrast, for the MFB results, pressure values were first filtered, and then the macro was

used. The average values of 100 cycles were not used for the MFB results, establishing the standard deviations.

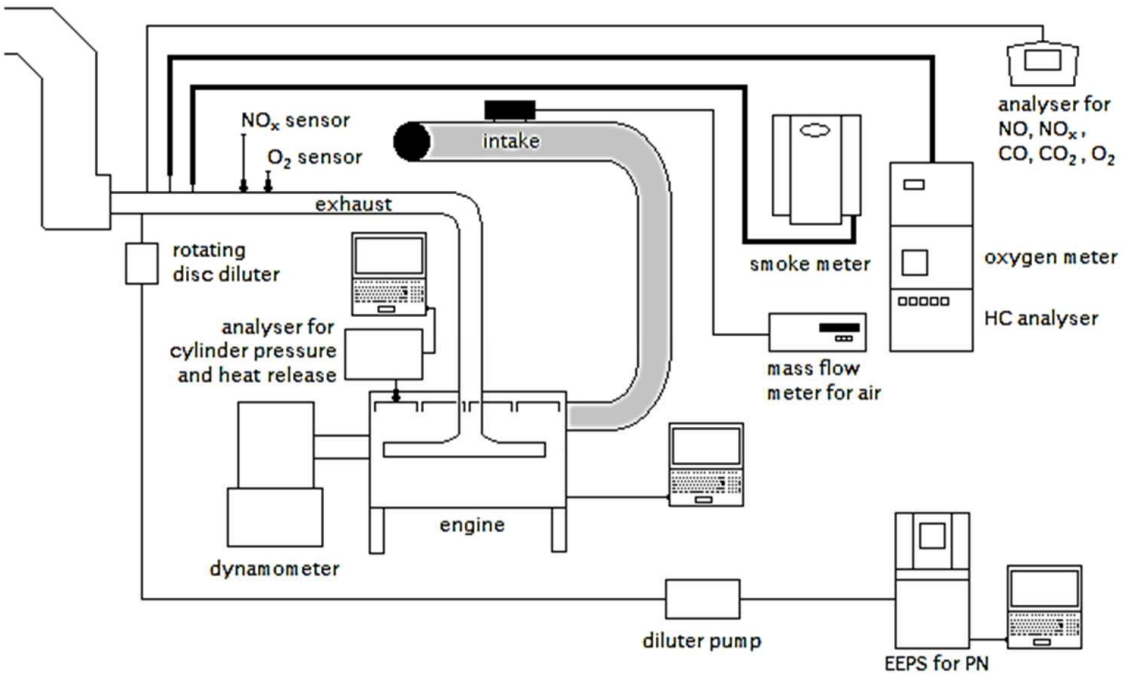

Figure 1. Engine measurement setup.

The exhaust temperatures were recorded by K type thermocouples (NiCu-NiAl). Air and exhaust pressures were determined by industrial transmitters. The engine airflow was measured by an ABB Sensyflow FMT700-P meter. Exhaust emissions were determined using the instruments listed in Table 4. The measured concentrations of gaseous emissions were used to calculate the brake specific emissions according to the ISO 8178 standard. (EN ISO 8178-2:2008).

Table 4. Instruments for emission measurements

Parameter	Analyser	Technology	Accuracy*
CO	TSI CA-6203 CA-CALC	Electrochemical	0–100 ppm: ±10% 100–5,000 ppm: ± 5%
O2	Siemens Oxymat 61	Paramagnetic	± 0.25%
NO, NOx	TSI CA-6203 CA-CALC	Electrochemical	0–100 ppm: ±10% 100–4,000 ppm: ± 5%
HC	J.U.M. VE 7	HFID	0–100,000 ppm: ±1%
Smoke	AVL 415 S	Optical filter	± 5%
Particle number	TSI EEPS 3090	Spectrometer	-

* Accuracy provided by the manufacturer.

An engine exhaust particle sizer (EEPS, model 3090, TSI Inc.) was used to determine the TPN within a particle size range of 5.6 to 560 nm. The exhaust sample was first diluted with ambient air by a rotating disc diluter (RDD - model MD19-E3, Matter Engineering AG), which had a constant dilution ratio of 60:1. Dilution air was kept at 150 °C while the exhaust aerosol sample was conducted to the RDD. The diluted

sample (5 L pm) was further diluted by purified air with a dilution ratio of 2:1. Thus, the total dilution ratio was 120:1.

TPN was recorded for three minutes per load point using the EEPS. The recorded data was processed with 'SOOT' inversion (Wang et al., 2016). The average TPN and the standard deviation of TPN values were calculated from the data with time intervals of 0.1 s.

Experimental matrix and measurement procedure

All measurements were performed under steady operating conditions without engine modifications. With high-viscosity FO, the default engine control parameters allowed the engine to run at an intermediate speed at engine loads of 50% or less, and at rated speed only at 10% load. Multistage injection (pilot, main and post injections) was used throughout the study. The results were compared to those of DFO. The experimental loads and engine speeds are set out in Table 5.

Table 5. Experimental loads

Engine speed (min^{-1})	2,200	1,500	1,500
BMEP (bar)	1.1	4.3	8.7
Load (%)	10	25	50

At the beginning of every measurement, the engine was warmed-up and the load was applied using DFO. The intake-air temperature was adjusted to 85 ± 1 °C downstream of the charge-air cooler to support auto-ignition of the fuels at each load. The temperature was controlled manually by regulating the flow of cooling water to the heat exchanger. The valve setting was kept constant. All measurements were taken only after the engine had stabilised, as determined by stability of the temperatures of coolant water, intake air and exhaust. The length of the measurement period was not tied to a certain time. With FO, the engine was started with DFO and after the engine had warmed up, the fuel was changed to FO. Both fuels were supplied at room temperature.

RESULTS AND DISCUSSION

This chapter shows the air temperature after the compressor of the turbocharger, exhaust gas temperature before turbocharger turbine, recorded injection parameters and results of cylinder pressure, heat release rate, mass fraction burned, combustion duration, gaseous and particulate emissions and smoke. The results obtained with FO are compared with those when using DFO and the differences are discussed.

Compressed air and exhaust gas temperatures

Fig. 2 presents compressed air temperature after the compressor of the turbocharger. Overall, the compressed air temperature after the turbocharger increased when engine load was increased, and it was higher at all loads with DFO compared to that of FO.

At low load, higher viscosity of FO compared to DFO result in poor atomization and dispersion of the fuel in the combustion chamber (Bhaskar et al., 2013). FO's high content of fatty acids is shown as late burning of these fractions, leading to higher exhaust gas temperature at low load at speed of 2,200 min^{-1} as shown in Fig. 3. However, at higher loads at engine speed 1,500 min^{-1}, exhaust gas temperature is lower with FO compared to DFO. The lowered exhaust gas temperature increases FO's brake thermal energy at higher loads, because more heat can be utilized during combustion process. (Bhaskar et al., 2013).

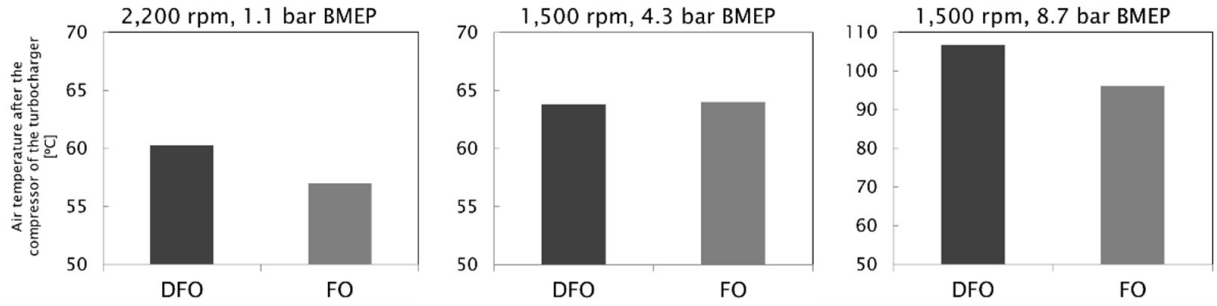

Figure 2. Air temperature after the compressor of the turbocharger.

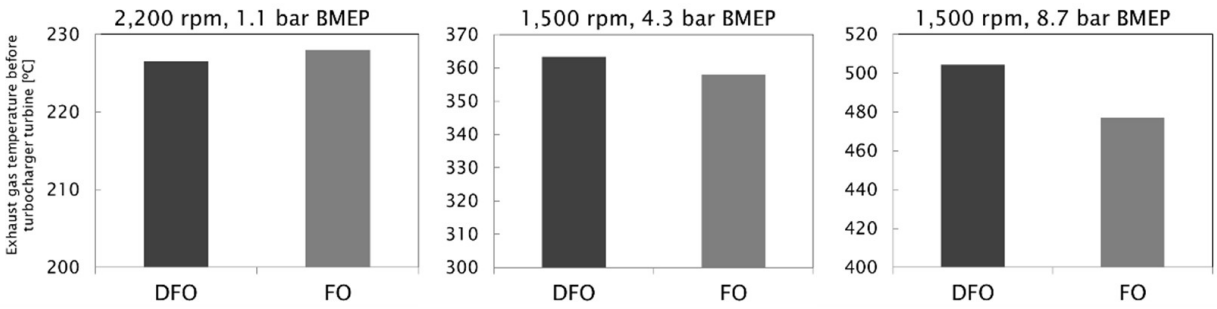

Figure 3. Exhaust gas temperature before the turbocharger turbine.

Injection parameters

For all test conditions, pilot and main injections were set before top dead centre (BTDC) and post injections occurred after top dead centre (ATDC). Exact timings and durations are shown in Table 6.

Table 6. Injection parameters for DFO and FO

Fuel	Speed	BMEP/ Load	Pilot Injection (ATDC)		Main injection (ATDC)		Post injection (ATDC)	
	min^{-1}	bar/%	Start °CA	Duration °CA	Start °CA	Duration °CA	Start °CA	Duration °CA
DFO	2,200	1.1/10	-18	4.6	-8	6.9	13	0
FO			-18	4.6	-8	7.6	13	0
DFO	1,500	4.3/25	-12	3.9	-4.5	8.2	13	4.7
FO			-11	3.9	-4.4	9.6	15	4.7
DFO	1,500	8.7/50	-8.7	3.5	-2.1	13	21	4.5
FO			-9.4	3.8	-2.5	16	22	3.4

Injection timings and durations were broadly similar with both fuels at 2,200 min^{-1}, but the duration of the main injection was longer for FO because its lower heating value is less than DFO's.

At the load of 4.3 bar BMEP and engine speed 1,500 min^{-1}, pilot injection started 1 °CA earlier with DFO compared to FO. The main injection started at the same time with both fuels but injection duration with FO was again longer than with DFO. FO's post injection started 2 °CA later than with DFO, most probably delayed due to FO's longer main injection duration. The duration of post injection was still similar for both fuels.

With FO at high load at 1,500 min^{-1}, pilot injection started earlier (9.4 °CA BTDC) than with DFO (8.7 °CA BTDC). An advanced injection may increase NOx emission (How et al., 2012; Shahabuddin et al., 2013) in comparison with fossil diesel. However, based on Heywood (2018), a longer pilot is used to shorten the ID of fuel by increasing in-cylinder temperatures for main injections. The main injection, started 0.4 °CA later with DFO and post injection started 1 °CA earlier with DFO. The duration of the main injection was longer with FO than with DFO.

The volumetric amount of injected fuel was assumed to correlate to injection durations because fuel injection was controlled according to load/speed requests. The longer main injection durations were due to higher viscosity and surface tension of FO, which increased the total injection duration due to decreased flow through the injector (Bae & Kim, 2016).

As expected, pilot injection duration increased when the engine load was reduced because the pilot is used especially at low loads to promote ignition, reduce ID and to smooth the increase of combustion pressure. Post injections are used to reduce particulate and soot emissions, primarily at lighter loads and lower engine speeds (Heywood, 2018). This technique was observed at 1,500 min^{-1}, where post-injection duration did increase when the engine load was reduced. However, at an engine speed of 2,200 min^{-1}, post injection duration was a short spike with both fuels.

Cylinder pressure

Injection timing, primarily affects maximum cylinder pressure (MCP). However, the pressure also depends on the burned fuel fraction during the premixed combustion phase, and thus on the ignition delay (ID). ID is a period when injected fuel entrains to cylinder, atomizes and mixes with existing air but does not yet ignite. Chemical reactions start slowly and ignition occurs after the ID. ID has a direct effect on the heat release rate and an indirect impact on engine noise and exhaust gas emission formation (Aldhaidhawi et al., 2017; Kuszewski, 2019). A long ID results in a rapid pressure increase in the combustion chamber when unburned fuel finally ignites. The rapid pressure increase leads to diesel knock, higher soot emissions, malfunctions in engine operation and engine damages (CIMAC, 2011; Ogawa et al., 2018; Hissa et al., 2019; Kuszewski, 2019). A longer ID and more fuel burned in the premixed phase usually results in a steeper pressure rise and higher MCP (Hissa et al., 2019).

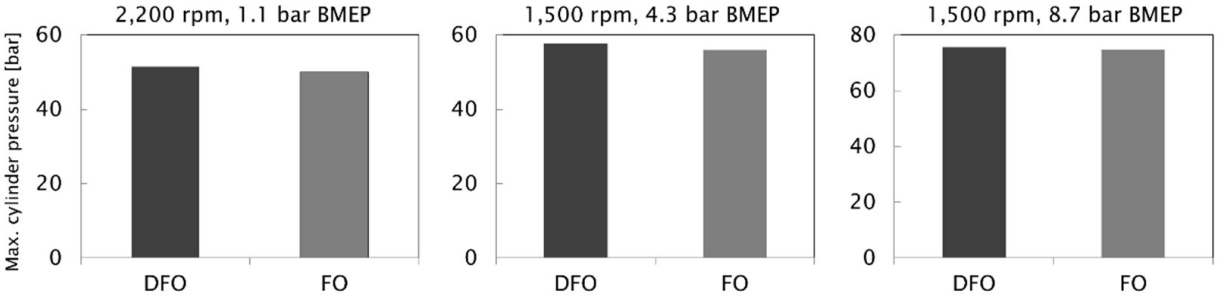

Figure 4. Maximum cylinder pressures at rated and intermediate speeds.

Fig. 4 shows that MCP values with DFO were slightly higher than with FO at all studied load points. The differences between DFO and FO increased with the load.

The averaged MCP values and their standard deviations of 100 consecutive cycles are given in Table 7.

Table 7. Maximum cylinder pressures and standard deviations

Fuel	Speed min^{-1}	BMEP/ Load bar, %	Max. cylinder pressure (avg) bar	StDev (filtered)
DFO	2,200	1.1/10	51	0.08
FO			50	0.05
DFO	1,500	4.3/25	58	0.12
FO			56	0.07
DFO	1,500	8.7/50	76	0.13
FO			75	0.06

Heat release rate (HRR)

Combustion starts with a rapid burning phase that lasts only a few CA degrees and produces the first spike in the HRR curve. It is followed by the main heat-release period with a longer duration and a more rounded profile. The tail of the HRR curve is the remainder of the fuel's chemical energy released when burned gases mix with excess air that was not involved in the main combustion. (Heywood, 2018) Figs 5–7 show HRR curves for the studied fuels. A slight loss observed at the beginning of each HRR curve is due to the heat transfer into the liquid fuel for vaporising and heating (Heywood, 2018).

Fig. 5 illustrates the HRR of two fuels at 2,200 min^{-1} and 1.1 bar BMEP. The FO curve indicates that its pilot did not ignite properly, so FO had a higher peak HRR compared to DFO. FO's peak also occurred a few crank angle degrees later than DFO's.

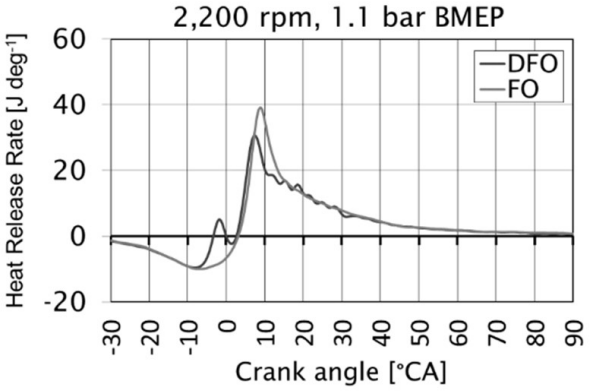

Figure 5. Heat release rate curves with FO and DFO at 2,200 min^{-1} and 1.1 bar BMEP.

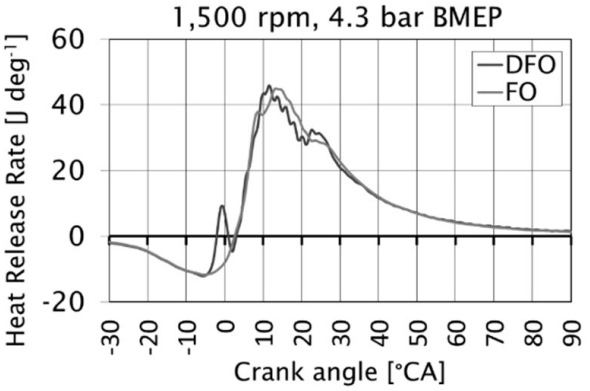

Figure 6. Heat release rate curves with FO and DFO at 1,500 min^{-1} and 4.3 bar BMEP.

Fig. 6 depicts the two HRR curves at 1,500 min^{-1} and 4.3 bar BMEP. The HRR of DFO again shows a clear initial HRR peak and even an increase in the HRR at post-injection. In contrast, the FO curve shows no clear HRR peaks from either pilot or post injections, and its general profile is more rounded than DFO curve. Most likely, the high viscosity and surface tension of FO increased the droplet size of the fuel spray, impairing ignition. FO's lower CN would also increase ignition delay leading, to retarded combustion (Bae & Kim, 2016; Heywood, 2018; Hissa et al., 2019). However, the lower compressibility and higher oxygen content of FO may have accelerated the HRR of FO (Shahabuddin et al., 2013).

Fig. 7 shows the two HRR curves when the load at 1,500 min^{-1} increased to 8.7 bar BMEP. Now, the FO's HRR peak from the pilot injection is clearly evident but is still seen later than that of DFO. FO shows no post-injection peak but seemed to burn slightly faster than DFO in the later phase of combustion. Again, the high viscosity and surface tension of FO increased the size of fuel droplets, and the time required to evaporate the fuel droplets also increased.

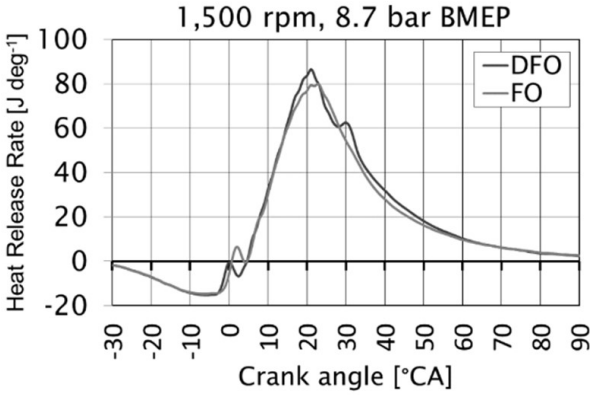

Figure 7. Heat release rate curves with FO and DFO at 1,500 min^{-1} and 8.7 bar BMEP.

Mass fraction burned (MFB)

In the current study, the maximum compression pressure was at two degrees CA before the top dead centre at an engine speed of 1,000 min^{-1}. This had no effect on measured results but must be taken into consideration when the results are examined.

Table 8 presents mass fraction burned (MFB) values with their standard deviations. MFB values were very similar with both fuels. Only at MFB 90% at 2,200 min^{-1} was there more than 1 °CA of difference between them. Both fuels showed MFB 50% at between 24 to 26 °CA at lower loads and at 29 °CA at higher load. Most probably, FO burned slightly more rapidly due to its oxygen content after a shade slower ignition.

Table 8. Mass fraction burned and standard deviations

Fuel	BMEP/Speed bar min^{-1}	MFB 10% °CA	StDev	MFB 50% °CA	StDev	MFB 90% °CA	StDev
DFO	1.1/2,200	12	0.41	24	0.75	65	4.3
FO		13	0.46	25	0.78	69	4.3
DFO	4.3/1,500	13	0.21	25	0.31	59	1.5
FO		14	0.17	26	0.24	58	1.4
DFO	8.7/1,500	18	0.17	29	0.26	58	1.2
FO		18	0.13	29	0.24	59	1.3

Combustion duration

Combustion duration (CD) can be defined either as the time interval between MFB 5% and MBF 90% (Fig. 8) or the time interval between MFB 10% and MFB 50% (Fig. 9).

The high viscosity and surface tension of FO generated larger droplets. Larger droplets, again, require more time to evaporate and burn (Heywood, 2018). Fig. 8 shows that at 1.1 BMEP at 2,200 min^{-1} and at 8.7 bar BMEP at 1,500 min^{-1}, CD 5–90% was longer with FO than with DFO. However, FO's high oxygen content may have improved combustion by decreasing combustion duration since CD 10–50% was shorter or equal with FO compared to DFO (Fig. 9).

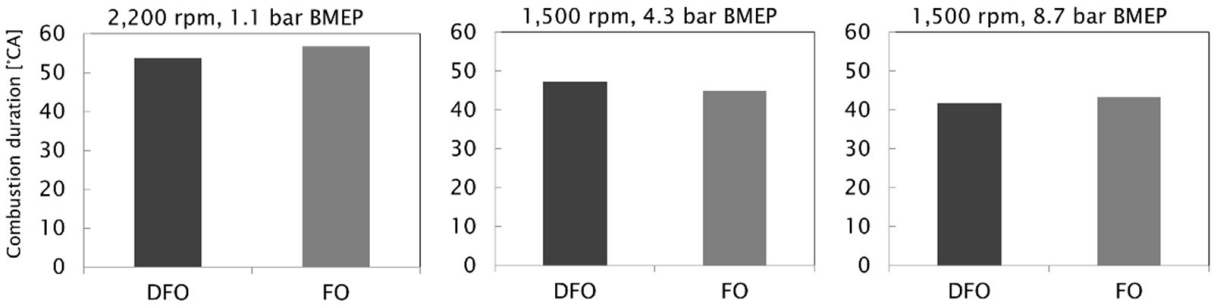

Figure 8. Combustion duration (°CA) at all engine loads, determined as crank angles between MFB 5% and MFB 90%.

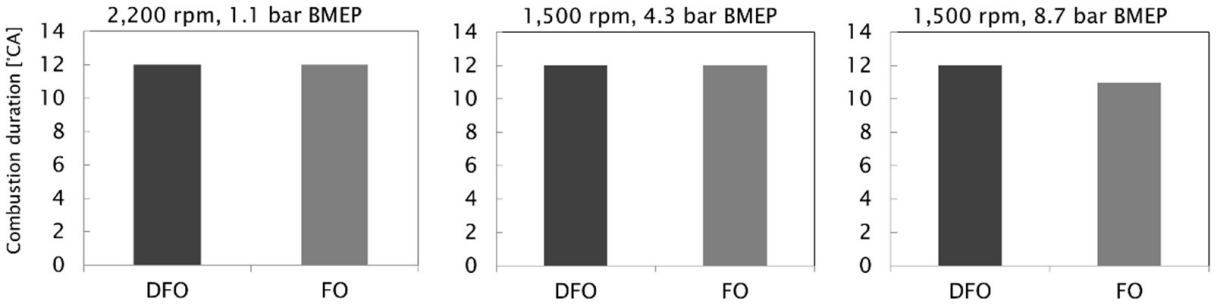

Figure 9. Combustion duration (°CA) at all engine loads, determined as crank angles between MFB 10% and MFB 50%.

Gaseous emissions, smoke and total particle numbers (TPN)

Fig. 10 illustrates the brake-specific emissions of NOx, CO, and HC. The smoke numbers are shown in Fig. 11 and total particle numbers (TPN) are depicted in Fig. 12.

In broad terms, combustion of FO generated more NOx, CO and HC than when using DFO, but the difference between the fuels diminished when the engine load was increased.

At 1,500 min^{-1}, FO emitted very similar NOx emissions of 2.6 g kWh^{-1} at both loads. The result at the higher speed was 4.0 g kWh^{-1}. Compared with DFO, FO increased NOx by 23% at lower load at 1500 min^{-1} while at higher load the difference was only 2%. However, at 2,200 min^{-1} at 1.1 bar BMEP, DFO showed 21% higher NOx than FO. The higher NOx for FO may be due to the presence of molecular oxygen that promoted oxidation of nitrogen (Shahabuddin et al., 2013). Later ignition and increased premixed combustion may also have affected NOx formation (Satyanarayana & Muraleedharan, 2012).

Less excess air and higher combustion temperature promoted NOx formation. As seen in Fig. 10, increased engine load improved fuel-air mixing and fuel oxidation. The improved mixing rate led to a reduction in CO, HC and smoke as engine load was increased. It is most likely that inadequate spray formation of FO caused higher NOx, CO and HC emissions (Niemi et al., 2009).

FO produced more CO than DFO at all loads. At 1,500 min^{-1} at the lower load, CO was 2.2 g kWh^{-1} for FO and 0.52 g kWh^{-1} for DFO. At higher load, FO emitted 0.96 g kWh^{-1} and DFO 0.40 g kWh^{-1}. At 2,200 min^{-1}, CO emissions from FO were very high at, 23 g kWh^{-1} while DFO generated approximately 3 g kWh^{-1}. FO's high CO emissions indicate poor fuel-air mixing and incomplete combustion, especially at very

low loads. Ollus & Juoperi (2007) reported that liquid biofuel (LBF) increased CO emissions in a medium-speed diesel engine, and one reason for increase may be that there have been some cold regions in the combustion chamber causing a disturbance of combustion process. Satyanarayana & Muraleedharan (2012) also report on poor atomisation and incomplete combustion when unheated palm oil of high viscosity was used as engine fuel. However, reduced CO formation was reported when the neat oil was preheated.

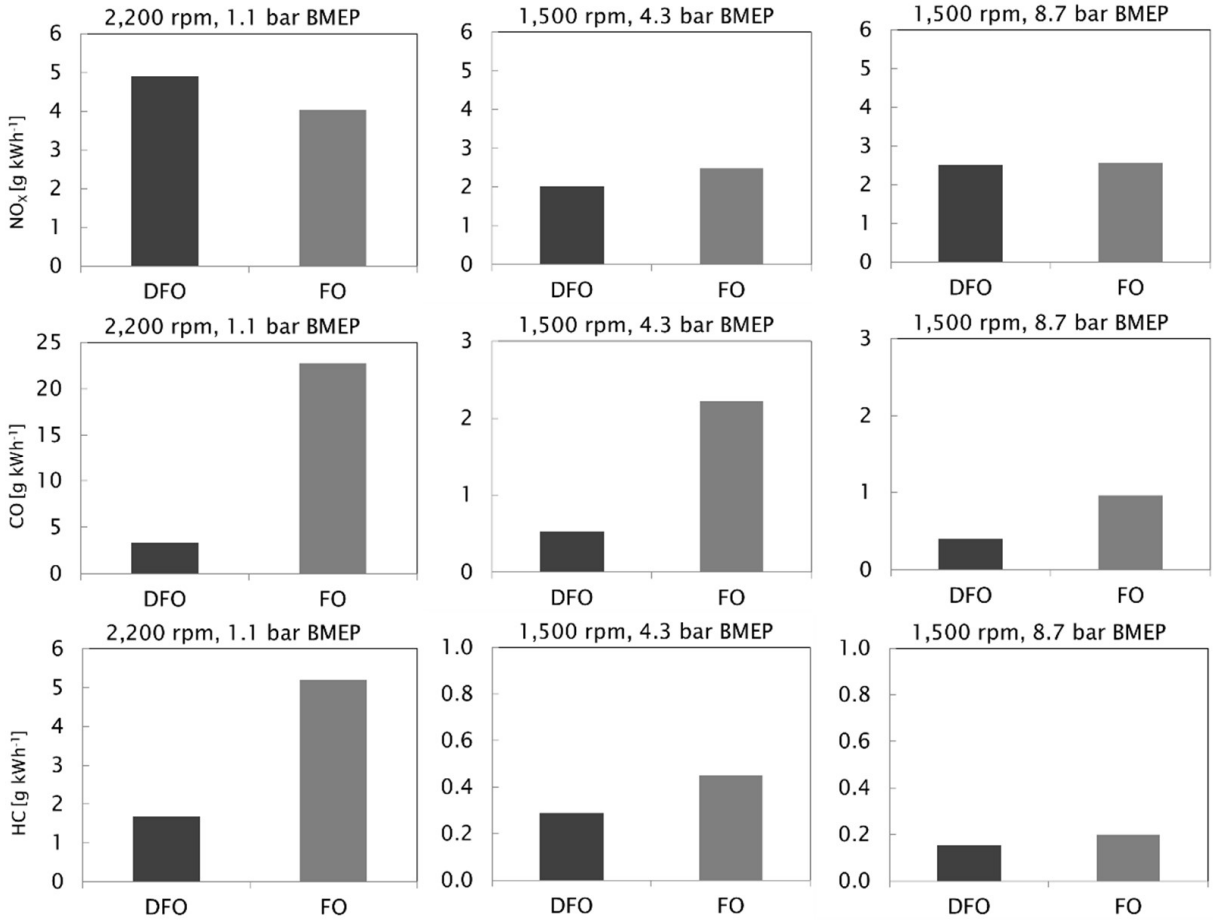

Figure 10. Brake specific emissions of NOx, CO and HC for FO and DFO.

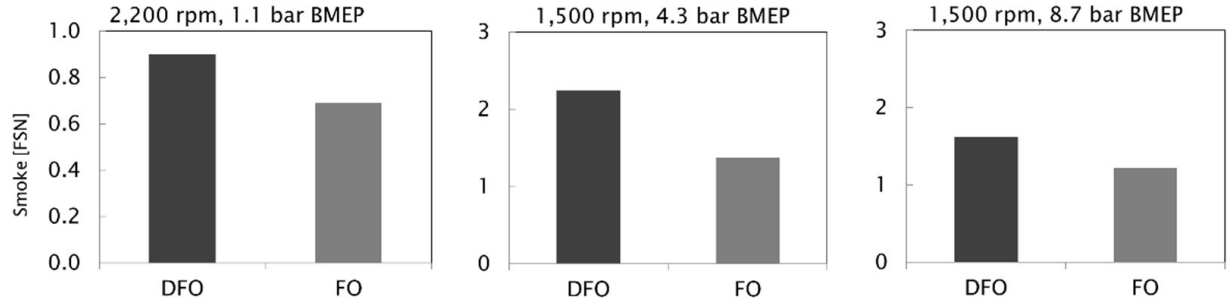

Figure 11. Smoke numbers for FO and DFO.

HC emissions also increased clearly when FO was burned instead of DFO, confirming that air-fuel mixing and combustion with FO was inferior at these rather low loads. At 1,500 min^{-1} at the lower load, HC was 0.45 g kWh^{-1} for FO and 0.29 g kWh^{-1} for DFO. At higher load, FO emitted 0.20 g kWh^{-1} and DFO 0.15 g kWh^{-1}. At 2,200 min^{-1}, HC was again high for FO at 5.2 g kWh^{-1} while DFO generated 1.7 g kWh^{-1}. Our HC (and CO) results correspond with those of Hoang (2019). Hoang (2019) studied preheated neat coconut oil in a diesel engine and detected higher CO and HC emissions compared to DFO. The reason given was the incomplete combustion of the coconut oil. Satyanarayana & Muraleedharan (2012) also observed an increase in HC emissions with neat vegetable oils compared to DFO. Turunen & Niemi (2002) explain higher HC emissions at lower engine loads compared to higher loads due to lean mixture areas, where fuel-air mixture ignites and burns poorly. Slow fuel injection speed may also increase HC emissions. Another clear source for HC emissions in diesel engine, is the sac inside an injection nozzle. The sac storages fuel after injection, the fuel evaporates slowly through nozzle holes and is not participated to combustion (Turunen & Niemi, 2002).

Contrary to CO and HC, smoke decreased at all loads with FO. At speed of 2,200 min^{-1} and 1.1 bar BMEP, FO generated 0.7 FSN, whereas the smoke reading for DFO was 0.9 FSN. At 4.3 bar BMEP at 1,500 min^{-1}, FO's smoke number was 1.4, and at high load 1.2 FSN. The corresponding values for DFO were 2.2 FSN and 1.6 FSN. Niemi et al. (2009) also observed improved smoke for crude fish oil compared to DFO in a high-speed diesel engine, concluding that, the most probable reason was the high oxygen content of biofuels. Highly oxygenated fuels produce less smoke due to higher flame temperature and lower radiative heat losses in the cylinder (Chauhan et al., 2010; Shahabuddin et al., 2013).

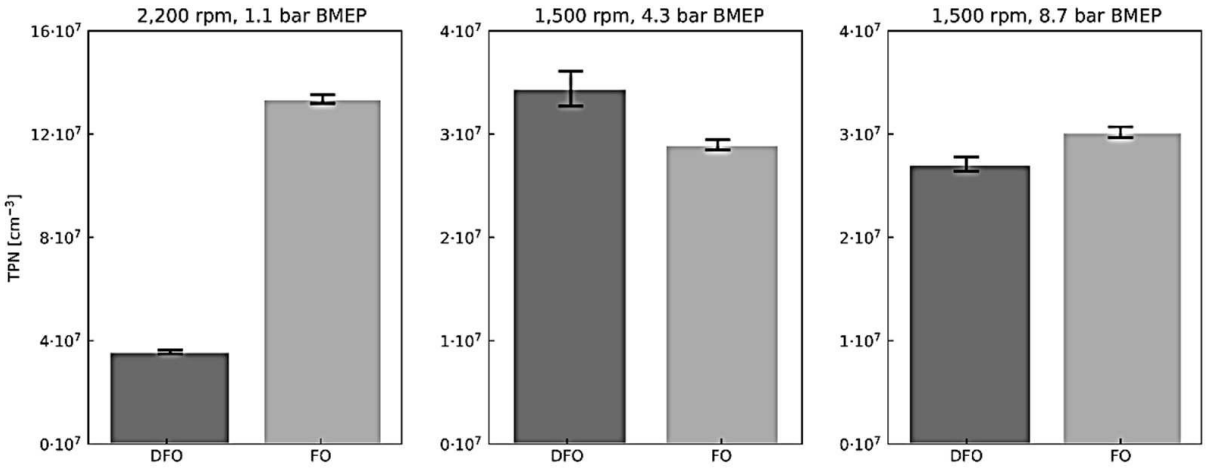

Figure 12. TPN emissions with FO and DFO at all loads and speeds.

Fig. 12 shows the TPN emissions with FO and baseline DFO at all loads and speeds. Each bar denotes the TPN mean and error bars represent the standard deviation of TPN during the measurement period of three minutes. At 4.3 bar BMEP load at 1,500 min^{-1}, FO reduced TPN, but the other loads the order of fuels was the opposite. Compared to the DFO baseline, FO emitted more particles at 8.7 bar BMEP at 1,500 min^{-1}. The greatest difference was at low load at 2,200 min^{-1}, where FO's TPN was 3.7 times higher

than DFO's. The TPN did not improve at all load conditions with FO compared to DFO although the smoke did. A reduction in PM emissions can be expected if the sulphur content, density, viscosity and carbon-to-hydrogen ratio of the fuel are reduced (Nabi et al., 2012).

On the contrary, soot emission may increase along with fuel viscosity because high viscosity can lead to less favourable fuel atomisation and hence combustion may not be completed. (Kegl et al., 2013; Nabi et al., 2012). High fuel density may inhibit fuel spray formation during fuel injection, potentially causing incomplete fuel burning and high emissions. (Hissa et al., 2018). In this study, FO´s sulphur content of 2.1 mg kg^{-1} was less than DFO´s sulphur content of 3.3 mg kg^{-1}. Density at 15 °C was higher for FO (920 kg m^{-3}) compared to that of DFO (835 kg m^{-3}). Moreover, the FO had higher kinematic viscosity (28 mm^2 s^{-2}) than DFO (3 mm^2 s^{-2}). The carbon-to-hydrogen ratio of FO (0.56) was also higher than that of DFO (0.53). With the exception of sulphur, these differences in the density, viscosity, and carbon-to-hydrogen ratio that were all higher for FO may explain the high TPN of FO at low load at rated speed and at high load at intermediate speed.

Unlike our study, several other studies have shown improvements in emissions performance with crude bio-oils. Preheating the bio-oil has reduced exhaust emissions further and increased the engine power output by lowering the high viscosity of neat bio-oils to a level, comparable with DFO (Hoang, 2019). The high viscosity can also be lowered by blending bio-oil with lower viscosity fuel or processing the oil through the transesterification method to produce biodiesel (Chauhan et al., 2010). However, a manufacturer of large engines does not recommend blending crude bio-oils (Ollus & Juoperi, 2007). Further progress for FO should include optimisation of injectors and injection settings and preheating fuel to improve fuel-air mixing, decrease ID and improve combustion.

CONCLUSIONS

Crude fish oil (FO) at room temperature was investigated in a high-speed, off-road diesel engine. The engine was turbocharged, intercooled, and equipped with a common rail injection system and 6-hole high flow rate injectors. Measurements were made at two loads at intermediate speed and at one load at rated speed. The results were compared to those of DFO.

The FO was classified as waste and could not safely be used in, for example, food production. It was produced from local waste sources at moderate cost. Generally, these kinds of renewable fuels are seen as one alternative for fossil fuels when targeting at reduction of greenhouse gas emissions.

Based on the results, the following conclusions could be drawn:

– The high viscosity and surface tension of FO inhibited fuel spray formation and air-fuel mixing.

– This and the low cetane number of FO, increased ignition delay and hindered ignition resulting in incomplete combustion.

– Consequently, NOx, CO and HC emissions increased compared with DFO.

– Smoke, however, decreased with FO.

– Except at low load at 1,500 min-1, the TPN did not improve with FO compared to DFO. Density, viscosity, and carbon-to-hydrogen ratio were all higher for FO, so these differences may explain the high TPN with FO.

– Optimisation of the injection system and preheating the fuel are the main avenues towards improving engine performance and emissions with FO. Operation at very low loads most probably should also be avoided when using FO.

ACKNOWLEDGEMENTS. This project was one part of the national Future Combustion Engine Power Plant research program (grant number: 2804/31/2009). The authors wish to thank Business Finland for the financial support of the program.
The authors offer their appreciation to Ms. Katriina Sirviö, Mr. Olav Nilsson, Mr. Markus Uuppo Mr. Henri Huusko and Mr. Marko Vallinmäki for their kind assistance in the measurements.

REFERENCES

Adeoti, I.A. & Hawboldt, K. 2015. Comparison of biofuel quality of waste derived oils as a function of oil extraction methods. *Fuel* **158**, 183–190.

Aldhaidhawi, M., Chiriac, R. & Badescu, V. 2017. Ignition delay, combustion and emission characteristics of Diesel engine fueled with rapeseed biodiesel -A literature review. *Renewable and Sustainable Energy Review* **73**, 178–186.

Bae, C. & Kim, J. 2016. Alternative fuels for internal combustion engines. *Proceedings of the Combustion Institute* **0000**, 1–5.

Bhaskar, K., Nagarajan, G. & Sampath, S. 2013. Optimization of FOME (fish oil methyl esters) blend and EGR (exhaust gas recirculation) for simultaneous control of NOx and particulate matter emissions in diesel engines. *Energy* **62**, 224–234.

Bosch GmbH. 2018. *Automotive Handbook*. 10th Edition, Robert Bosch GmbH, Karlsruhe, Germany. ISBN 978-1-119-53081-7, 1750 pp.

Bruun, N., Shoulaifar, T.K., Hemming, J., Willför, S & Hupa, L. 2019. Characterization of waste bio-oil as an alternate source of renewable fuel for marine engines. *Biofuels*. ISSN: 1759-7269. doi: 10.1080/17597269.2019.1628481

Chauhan, B.S., Kumar, N., Du Jun, Y. & Lee, K.B. 2010. Performance and emission study of preheated Jatropha oil on medium capacity diesel engine. *Energy* **35**, 2484–2492.

Ching-Velasquez, J., Fernández-Lafuente, R., Rodrigues, R.C., Plata, V., Rosales-Quintero, A., Torrestiana-Sánchez, B. & Tacias-Pascacio, V.G. 2020. Production and characterization of biodiesel from oil of fish waste by enzymatic catalysis. *Renewable Energy* **153**, 1346–1354.

CIMAC, The International Council on Combustion Engines. 2011. Fuel quality guide – Ignition and combustion. 27 pp.

de Almeida, V.F., García-Moreno, P.J., Guadix, A. & Guadix, E.M. 2015. Biodiesel production from mixtures of waste fish oil, palm oil and waste frying oil: Optimization of fuel properties. *Fuel Processing Technology* **133**, 152–160.

Deshmukh, D., Madan Mohan, A., Anand, T.N.C. & Ravikrishna, R.V. 2012. Spray characterization of straight vegetable oils at high injection pressures. *Fuel* **97**, 879–883.

Drenth, A.C., Olsen, D.B., Cabot, P.E. & Johnson, J.J. 2014. Compression ignition engine performance and emission evaluation of industrial oilseed biofuel feedstocks camelina, carinata, and pennycress across three fuel pathways. *Fuel* **136**, 143–155.

EN ISO, 8178-2:2008. Reciprocating Internal Combustion Engines. Exhaust Emission Measurement; Part 2: Measurement of Gaseous and Particulate Exhaust Emissions under Feld Conditions; ISO: Geneva, Switzerland, 2008.

Esteban, B., Riba, J-R., Baquero, G., Rius, A. & Ruig, R. 2012. Temperature depence of density and viscosity of vegetable oils. *Biomass and Bioenergy* **42**, 164–171.

Fan, Y., Hashimoto, N., Nishida, H & Ozawa, Y. 2014. Spray characterization of an air-assist pressure-swirl atomizer injectiong high-visocity Jatropha oils. *Fuel* **121**, 271–283.

FAO. 2020. The State of World Fisheries and Aquaculture 2020. Sustainability in action. Rome. 244 pp. https://doi.org/10.4060/ca9229en

Heywood, J.B. 2018. *Internal Combustion Engine Fundamentals*, 2nd Edition, McGraw-Hill Education, USA. ISBN 978-1-260-11610-6. 1056 pp.

Hissa, M., Niemi, S.& Sirviö, K. 2018. Combustion property analyses with variable liquid marine fuels in combustion research unit. *Agronomy Research* **16**(S1), 1032–1045.

Hissa, M., Niemi, S. & Sirviö, K. 2019. Ignition Studies of Liquid Marine Fuels with Different Ignition Analyzers. In *the 29th CIMAC World Congress*, Vancouver, Canada. Paper 121. 11 pp.

Hissa, M., Niemi, S. & Niemi, A. 2020. Combustion and emission studies of a common-rail direct injection diesel engine with various injector nozzles. *Agronomy Research* **18**(3), 2033–2048. https://doi.org/10.15159/ AR.20.165

Hoang, A.T. 2019. Experimental study on spray and emission characteristics of a diesel engine fueled with preheated bio-oils and diesel fuel. *Energy* **171**, 795–808.

How, H.G., Teoh, Y.H., Masjuki, H.H. & Kalam, M.A. 2012. Impact of coconut oil blends on particulate-phase PAHs and regulated emissions from a light duty diesel engine. *Energy* **48**, 500–509.

Jayasinghe, P. & Hawboldt, K. 2012. A review of bio-oils from waste biomass: Focus on fish processing waste. *Renewable and Sustainable Energy Reviews* **16**, 798–821.

Juoperi, K. & Ollus, R. 2008. Alternative fuels for medium-speed diesel engines. *Wärtsilä Tech. J.* **1**, 24–28.

Kegl, B., Kegl, M. & Pehan, S. 2013. *Green diesel engine. Biodiesel usage in diesel engines*. London: Springer-Verlag. 263 pp. ISBN 978-1-4471-5324-5

Kuszewski, H. 2019. Experimental investigation of the autoignition properties of ethanol-biodiesel fuel blends. *Fuel* **235**, 1301–1308.

Lin, C-Y & Li, R-J. 2009. Engine performance and emission characteristics of marine fish-oil biodiesel produced from the discarded parts of marine fish. *Fuel Processing Technology* **90**, 883–888.

Nabi, M.N., Brown, R.J., Ristovski, Z. & Hustad, J.E. 2012. A comparative study of the number and mass of fine particles emitted with diesel fuel and marine gas oil (MGO). *Atmos. Environ*. **57**, 22–28.

Niemi, S., Uuppo, M., Virtanen, S., Karhu, T., Ekman, K., Svahn, A., Vauhkonen, V., Agrawal, A. & Hiltunen, E. 2011. Animal Fat Based Raw Bio-Oils in a Non-Road Diesel Engine Equipped with a Diesel Particulate Filter. In Bartz, W.J. (ed) (2011): *8th International Colloquium Fuels; Conventional and Future Energy for Automobiles*. Ostfildern, Germany: Technische Akademie Esslingen, pp. 517–528.

Niemi, S., Vauhkonen, V., Hiltunen, E., Virtanen, S., Karhu, T., Ekman, K., Salminen, H. & Appelberg, S. 2009. Results of an Off-Road Diesel Engine Driven with Different Animal Fat Based Biofuels. In *ASME Internal Combustion Engine Division 2009 Fall Technical Conference*. Lucerne, Switzerland. ASME Paper ICEF2009-14010

Ministry of the Environment, Finland. 2019. Government's climate policy: carbon-neutral Finland by 2035. Available in: https://ym.fi/en/carbon-neutral-finland-2035.

Murtonen, T. 2004. Fuel quality effects on fuel consumption in a heavy-duty diesel engine. Project report PRO3/P5115/04. VTT Technical Research Centre of Finland Ltd. pp. 7. (in Finnish).

Ogawa, H., Morita, A., Futagami, K. & Shibata, G. 2018. Ignition delay in diesel combustion and intake gas conditions. *International Journal of Engine Research* **19**(8), 805–812.

Ollus, R. & Juoperi, K. 2007. Alternative fuels experiences for medium-speed diesel engines. In *The 25th CIMAC World Congress 2007*, Vienna, Austria. Paper 234, 15 pp.

Rakopoulos, D.C., Rakopoulos, C.D., Giakoumis, E.G., Papagiannakis, R.G. & Kyritsis, D.C. 2014. Influence of properties of various common bio-fuels on the combustion and emission characteristics of high-speed DI (direct injection) diesel engine: Vegetable oil, bio-diesel, ethanol, n-butanol, diethyl eter. *Energy* **73**, 354–366.

Satyanarayana, M. & Muraleedharan, C. 2012. Experimental Studies on Performance and Emission Characteristics of Neat Preheated Vegetable Oils in a DI Diesel Engine. *Energy Sources*, Part A: Recovery, Utilization, and Environmental Effects **34**, 1710–1722.

Shahabuddin, M., Liaquat, A.M., Masjuki, H.H., Kalam, M.A. & Mofijur, M. 2013. Ignition delay, combustion and emission characteristics of diesel engine fueled with biodiesel. *Renewable and Sustainable Energy Reviews* **21**, 623–632.

Sirviö, K. 2018. *Issues of various alternative fuel blends for off-road, marine and power plant diesel engines*. Dissertation, Acta Wasaensia 400, University of Vaasa, Finland. ISBN 978-952-476-805-4, 138 pp.

Skog, S-F., Nilsson, O. & Stam, U. 2013. Biofuels at fisheries industry – project report, serie R: Report 7/2013. Novia University of Applied Sciences, Finland. ISBN: 978-952-5839-78-4, pp. 38 (in Swedish).

Turunen, R & Niemi, S. 2002. Chapter 21 – Polttomoottorit, In Raiko, R., Saastamoinen, J., Hupa, M & Kurki-Suoni, I. (eds), *Poltto ja palaminen*, 2nd Edition. International Flame Research Foundation, Teknillistieteelliset akatemiat, Helsinki, Finland. ISBN 951-666-604-3, pp. 614–620.

Wang, X., Grose, M.A., Caldow, R., Osmondson, B.L., Swanson, J.J., Chow, J.C., Watson, J. G., Kittelson, D.B., Li, Y., Xue, J., Jung, H. & Hu, S. 2016. Improvement of Engine Exhaust Particle Sizer (EEPS) Size Distribution Measurement – II. Engine Exhaust Particles. *J. Aerosol Sci*. **92**, 83–94.